

Monitoring plant condition and phenology using infrared sensitive consumer grade digital cameras



Wiebe Nijland^{a,*}, Rogier de Jong^b, Steven M. de Jong^c, Michael A. Wulder^d,
Chris W. Bater^a, Nicholas C. Coops^a

^a Department of Forest Resources Management, Forest Sciences Centre, University of British Columbia, 2424 Main Mall, Vancouver, BC, Canada V6T 1Z4

^b Remote Sensing Laboratories, University of Zurich, Winterthurerstrasse 190, CH-8057 Zurich, Switzerland

^c Department of Physical Geography, Utrecht University, Utrecht, The Netherlands

^d Canadian Forest Service (Pacific Forestry Centre), Natural Resources Canada, 506 West Burnside Road, Victoria, BC, Canada V8Z 1M5

ARTICLE INFO

Article history:

Received 23 April 2013

Received in revised form 16 August 2013

Accepted 16 September 2013

Keywords:

Phenology

Plant health

Near sensing

Digital camera

Infrared

Greenness

ABSTRACT

Consumer-grade digital cameras are recognized as a cost-effective method of monitoring plant health and phenology. The capacity to use these cameras to produce time series information contributes to a better understanding of relationships between environmental conditions, vegetation health, and productivity. In this study we evaluate the use of consumer grade digital cameras modified to capture infrared wavelengths for monitoring vegetation. The use of infrared imagery is very common in satellite remote sensing, while most current near sensing studies are limited to visible wavelengths only. The use of infrared-visible observations is theoretically superior over the use of just visible observation due to the strong contrast between infrared and visible reflection of vegetation, the high correlation of the three visible bands and the possibilities to use spectral indices like the Normalized Difference Vegetation Index.

This paper presents two experiments: the first study compares infrared modified and true color cameras to detect seasonal development of understory plants species in a forest; the second is aimed at evaluation of spectrometer and camera data collected during a laboratory plant stress experiment. The main goal of the experiments is to evaluate the utility of infrared modified cameras for the monitoring of plant health and phenology.

Results show that infrared converted cameras perform less than standard color cameras in a monitoring setting. Comparison of the infrared camera response to spectrometer data points at limits in dynamic range, and poor band separation as the main weaknesses of converted consumer cameras. Our results support the use of standard color cameras as simple and affordable tools for the monitoring of plant stress and phenology.

© 2013 Elsevier B.V. All rights reserved.

1. Introduction

Monitoring plant condition and phenology is crucial for understanding relationships between climate variability, environmental conditions, vegetation health, and productivity. Plant phenology is directly related to climate variations, both intra-annually (Polgar and Primack, 2011) and annually (Cleland et al., 2007; Linderholm, 2006; Badeck et al., 2004). Furthermore, plant phenology and condition drive primary productivity and influence other ecosystem services, such as habitat use for many species, including insects (Bale et al., 2002), birds (Papeş et al., 2012), and large herbivores (Nielsen et al., 2003, 2010; Post and Stenseth, 1999; Sharma et al., 2009). The use of consumer-grade digital cameras is recognized as a cost-effective method to obtain high temporal resolution data

on vegetation processes (Richardson et al., 2009). In phenological research, studies have utilized cameras mounted on fixed locations (Bater et al., 2011a; Kurc and Benton, 2010; Nijland et al., 2012; Richardson et al., 2009) or publicly available webcam imagery (Graham et al., 2010; Ide and Oguma, 2010) to monitor vegetation changes. Because the cameras are ground-based, observations are restricted to individual plant or stand scales and are commonly referred to as 'near sensing' (Jongschaap and Booij, 2004). Despite the local scale of inquiry, these data provide a critical link to monitoring vegetation over larger areas through observational networks (Graham et al., 2010; Jacobs et al., 2009), satellite remote sensing (Hufkens et al., 2012; Zhang et al., 2003), or a combination of both (Badeck et al., 2004; Coops et al., 2012; Liang et al., 2011).

Information on vegetation development from satellite images commonly relies on indices which compare the reflectance of vegetation in multiple spectral regions. The most common indices utilize the differential response of vegetation in near infrared (NIR) and red (R) or other visible bands. The normalized difference

* Corresponding author. Tel.: +1 604 827 4429; fax: +1 604 822 9106.

E-mail address: irss.ubc@wiebenijland.nl (W. Nijland).

vegetation index (NDVI) ($NIR - R/NIR + R$) (Tucker, 1979) is the most commonly used index (Liang et al., 2011; Soudani et al., 2012). Many studies have successfully used ground based infrared or mixed-spectrum cameras to study plant health, vegetation cover, or vegetation vigor, such as in precision agriculture (Bauer et al., 2011; Huang et al., 2010; Knoth et al., 2010), ecology (Aber et al., 2009), and archeology (Verhoeven et al., 2009), among others. The studies focus mostly on the spatial domain, while few studies analyzed time-series of *IR* or mixed imagery (Lelong, 2008). Many long term near sensing phenology studies however, rely on indices of greenness, either $2G - RB$, excess greenness, or G/RGB , green chromatic coordinate (Richardson et al., 2007; Sonnentag et al., 2012; Woebbecke et al., 1995). The difference in usage between satellite versus ground-based systems has principally been driven by atmospheric and economic considerations. Both air- and space-borne remote sensing systems are influenced by atmospheric scattering in the blue and green range and therefore better results are often obtained using longer wavelengths such as red and *NIR*. Satellite sensors are designed for Earth observation and thus include *NIR* detection capabilities, while consumer cameras are designed for taking pictures of cats and thus resemble the human vision system which has considerable overlap between especially red and green sensitivity (Konica and Minolta, 1998; Poynton, 1995). Atmospheric scattering is of little concern for near sensing as the target and the sensor are spatially much closer and shorter wavelengths like blue and green are less affected because of the reduced path length. Secondly, near sensing approaches often utilize inexpensive consumer-grade sensors (digital cameras), which facilitate autonomous remote operation and establishment of observational networks covering significant geographical areas or environmental gradients (Bater et al., 2011). In contrast, sensors that can acquire *NIR* image data are inclined to be more expensive, reducing both their flexibility in deployment and quantity of units deployed. The differences between spectral characteristics and approaches of remote and near sensing systems raise questions about the compatibility of the two approaches (Coops et al., 2012; Fisher et al., 2006). Additional research is required to improve our understanding of how these data compare both spatially and temporally, as well as how they can capture varying degrees of plant stress.

In this paper we discuss the use of single-capture infrared images for monitoring phenology and plant health. To do so we undertake two case studies, the first of which compares the performance of *IR* and true color cameras to detect seasonal development of understory plant species within a forest canopy. In contrast to the theoretical advantage of *IR* based systems, true color cameras outperform the *IR* converted sensors. Therefore, we use the second study to further explore response of *IR* and true color cameras to changes in plant health in a controlled laboratory environment. This study combines images and spectrometer data of a 52 day stress experiment on *Buxus sempervirens* plants. We use the spectrometer data to simulate the response of different camera systems to changes in plant health to help explain the performance of standard and converted consumer cameras in vegetation studies. Our main objective is evaluating the utility of consumer grade digital cameras, specifically with infrared conversions, for vegetation monitoring and phenology studies.

2. Methods

2.1. Infrared conversion of consumer-grade digital cameras

Consumer-grade digital cameras are fitted with either a CCD (charge coupled device) sensor or a CMOS (complementary metal-oxide-semiconductor) sensor. The silicon-based sensor substrate is generally sensitive to wavelengths between 350 nm and 1100 nm, including ultraviolet (UV) and *NIR* (Brooker, 2009). To obtain

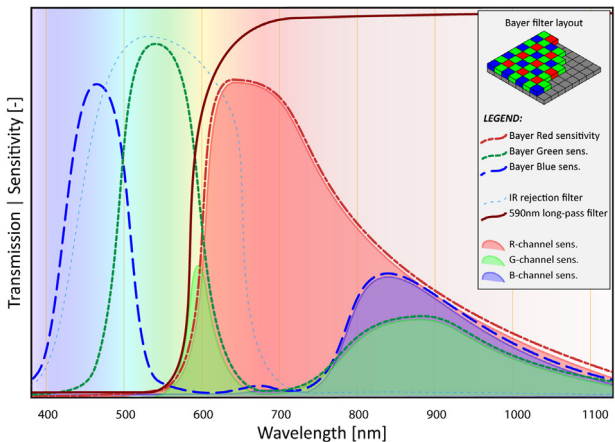


Fig. 1. Idealized filter profiles (lines) and channel sensitivity (surface) for camera with internal *IR* rejection filter replaced by a 590 nm long pass filter (after: LDP 2012, Nijland, 2012; Buil, 2012).

true-color images, most sensors have a Bayer color filter array (Bayer, 1976; Hirakawa and Wolfe, 2008), which combines a blue, a red and two green sensor cells into one true-color image pixel (Fig. 1). However, the filter materials (partly) transmit UV and *IR* radiation and therefore the cameras are fitted with a rejection filter that cancels out these wavelengths. It becomes possible to use standard CCD/CMOS sensors for *IR* imaging if the rejection filter is removed. A number of companies offer such conversions (e.g. Life Pixel Infrared Conversion Services, Mukilteo WA (www.lifepixel.com); LDP LCC, Carlstadt, NJ (www.maxmax.com)), or market purpose built digital cameras that are based on converted *RGB* sensors (Tetracam Inc, Chatsworth CA (www.tetracam.com)). The *IR* rejection filter is replaced by a filter that allows transmittance of *IR* and selected regions of the visible spectrum. The Bayer color filter array, on the other hand, is fused to the sensor substrate and cannot be removed. As a result, when using *RGB* cameras with the *IR* filter removed, the transmission profiles of the Bayer color channels remain, and depending on the filter choice each channel is sensitive to its original color and/or to *IR* radiation. Fig. 1 shows the sensitivity of a camera with the *IR* rejection filter replaced by a 590 nm long-pass filter. In this example, the *R*-channel records *Red + IR*, the *G*-channel records *IR* plus some component of the *Green*, and the *B*-channel records *IR* only. Other available long-pass filters include:

- Blue rejection filter (550 nm long-pass) giving $R = \text{Red} + \text{IR}$, $G = \text{Green} + \text{IR}$, $B = \text{IR}$ -only, such as in the Tetracam ADC (Tetracam 2011 (ADC manual, v.2.3)).
- *IR* only filter (>700 nm long pass), giving *IR*-only sensitivity to all channels, but with a wider range in *R* (700–1100 nm) than in *B* and *G* (800–1100 nm).
- Monotone *IR* only filter (>800 nm long pass), giving a more closely balanced sensitivity between the *RGB* channels at the cost of some spectral range (800–1100 nm).

A different type of filter for vegetation research is a dual-band-pass filter that transmits light only in the 400–600 nm and 700–800 nm ranges, giving $R = \text{IR}$ -only (700–800 nm), $G = \text{green}$, and $B = \text{blue}$ (LDP LCC, 2012).

The filter choice influences the spectral sensitivity and dynamic range of the sensor. A low cutoff wavelength gives better separation between the color bands and thus allows for using these color differences in calculating band indices. However, these filters often result in a large exposure difference between *R*, *G* and *B*, requiring exposure compensation and causing loss of usable dynamic



Fig. 2. Examples of images acquired at the botanical garden at UBC in *RGB* (left) and *IR-590* (right). The numbered rectangles identify species of interest (corresponding to Table 1).

range. In addition to their confounded spectral response, digital *RGB* cameras have a limited dynamic range and acquire images using automated exposure control setting which may involve in-camera image preprocessing; usually, this preprocessing cannot be tuned. As a result, band ratio indices have to be used to negate changes in brightness and exposures, such as the excess greenness ($2G - RB$) or green chromatic coordinate (G/RGB) in standard color images. With long-pass filters that transmit (a part of) red light (Fig. 1), indices that leverage the difference between the B (*IR-only*) and R ($Red + IR$), like the blue channel chromatic coordinate ($IR - B/IR - RGB$), are most promising. Additionally, the green channel may be used, although it has less potential due to its dual sensitivity in both the green and *IR* regions. Since the Bayer red pixels are by design sensitive for red and infrared light, it is not possible to obtain separate measurements of red and infrared with a single exposure. This, in turn, makes it impossible to calculate a true NDVI from a single image.

2.2. Field experiment

One *IR* and one *RGB* camera were installed at a field site in the University of British Columbia (UBC) botanical gardens in Vancouver, Canada. The field of view of the cameras covered nine species of interest including conifers, broadleaf evergreens, and deciduous plants and trees (Fig. 2). To assess the temporal consistency across the time series, we used brightness values from a wood-chip path as a plant-free surface with constant reflectance over the whole season. The cameras were setup before the start of the spring green-up in 2012 on April 4, and were taken down when the deciduous species had lost most of their leaves (November 8). In total, 6851 images were acquired, predominately from April to September.

The camera set was manufactured by Harbortronics (Fort Collins, Colorado, USA) and consisted of two commercially available Pentax K100D camera units. The Pentax K100D is a single-lens reflex (SLR) camera with a 6.1 megapixels CCD sensor and was, for this study, equipped with a 18–55 mm lens set to 18 mm. The two cameras recorded true-color *RGB* and *IR* respectively, the latter using a 590 nm long-pass filter. Both cameras were controlled by an intervalometer and sealed in a fiberglass housing. The entire system is self-contained and can operate unattended for several months, until available data storage is exhausted (Bater et al., 2011a). The system was mounted on a nearby tree, with the cameras as close to each other as possible. The intervalometers were configured to record hourly pictures during daytime (0900–1800 h). We used a manually fixed focus and automatic

exposure, with a compensation of minus two stops for the *IR* camera to compensate for changes in sensitivity introduced by the conversion. The white balance was fixed at 5500 K with tint + 10 (this sets the green–magenta balance) for the *RGB* images, and at 2400 K with tint at –70 for the *IR* images. Digital images were archived in RAW format to retain maximum data fidelity (Verhoeven, 2010), and ancillary data included a time stamp for acquisition reference. In addition to the image acquisition, the field sites were visited throughout the season to record phenological stages according to Dierschke (1972), from the phenolgy record we use the timing of leaf out and fall senescence (Table 1).

The image data was analyzed by extracting the color information from the images within areas of interest (Fig. 2) positioned on each of the species of interest (Table 1). For the *RGB* images we utilized the uncorrected green channel intensity (G) calculated the green chromatic coordinate ($G/R+G+B$) and the excess greenness ($2G - R+B$). From the *IR* images we extracted the blue band intensity (IR_B), the blue band chromatic coordinate ($IR_{Bx} = IR_B/IR_R + IR_G + IR_B$), excess IR_B intensity ($2IR_B - IR_R + IR_G$) and a pseudo NDVI ($((IR_{Bx} - IR_{Rx})/(IR_{Bx} + IR_{Rx}))$). A correlation matrix was calculated for all band indices and for all species of interest to select the indices with the strongest relations for further examination. We use salal (*Gaultheria shallon*) as an example of evergreen species, bog blueberry (*Vaccinium uliginosum*) as a deciduous example, and the wood path as constant reference surface.

2.3. Laboratory experiment

To examine the sensitivity for changes in plant phenology in a controlled environment with constant illumination, we acquired a series of images of potted *B. sempervirens* plants. In total, 18 plants were used and were divided into 6 groups, one control group and five stress groups, each receiving different treatments to investigate the effect of stress conditions on plant reflectance and appearance; an extensive analysis of the spectral data was published in de Jong et al. (2012). The six groups were treated as follows: (1) control, adequate care; (2) saturation, roots submerged in water; (3) light deprivation, kept in total darkness; (4) drought, plants received no water at all; (5) drought and heat, plants received no water and were subject to intense lighting from a halogen lamp for 8 h a day; (6) chlorine poisoning, normal watering was given with a 1.2% active chlorine solution.

The experiment continued for 52 days. At regular intervals, the spectra of all plants were measured using the portable spectroradiometer analytical spectral device (ASD) FieldSpec Pro JR, which has a spectral range of 350–2500 nm divided over three

Table 1

Species in the field of view of the camera, numbers refer to the annotation in Fig. 2.

	Binomial name	Common name	Leaf out >50%	Leaf fading >50%
1	<i>Vaccinium ovalifolium</i>	Alaska blueberry	2012-05-11	2012-10-11
2	<i>Vaccinium uliginosum</i>	Bog blueberry	2012-04-26	2012-11-08
3	<i>Ribes sanguineum</i>	Flowering currant	2012-04-26	2012-10-11
4	<i>Gaultheria shallon</i>	Salal	(leaf flush:2012-06-15)	–
5	<i>Viburnum edule</i>	Highbush cranberry	2012-04-26	2012-10-11
6	<i>Lysichiton americanus</i>	Skunk cabbage	2012-04-13	2012-08-09
7	<i>Betula pumila</i>	Bog birch	2012-05-11	2012-10-11
8	<i>Picea mariana</i>	Black Spruce	–	–
9		Wood Path	–	–

sensors and a sampling width of 1.5 nm (350–1000 nm) or 2.0 nm (1000–2500 nm) (ASDI, 2011). It has an 8° field of view optical lens, which is attached through a fiber-optic cable. A dark and a bright reference target were placed in all images to provide a fixed white-balance and exposure in each image. On days 8, 37, and 52 the plants were photographed under controlled lighting conditions and with constant photo geometry and plant orientation. Photos were taken with a Canon EOS 350D DSLR camera (Canon Inc, Japan): one in standard RGB color, and one with a converted camera employing a 715 nm long-pass infrared filter. Images were acquired with a fixed exposure and with manual settings to ensure constant settings over the whole time series. The camera and plant set up is shown in Fig. 3. From the photos we extracted the average response over the whole plant (excluding the pot) and surrounding scene elements, except for minor parts of the neutral background.

We simulated the responses of different camera filters to changes in plant health using the ASD spectra and theoretical camera response curves. The simulations were used to assess the effect of different filter configurations separated from issues related to the exposure and processing of images. The simulations were made with seven different configurations: Standard camera IR-rejection filter (normal RGB, Fig. 4); uniform 100 nm RGB; 590 nm long-pass filter (Fig. 1); 715 nm long-pass filter; 830 nm long-pass filter; red rejection dual band pass filter (Fig. 4);

and Thematic Mapper bands 4, 3, and 2 (Markham and Helder, 2011) (G 0.52–0.60; R 0.63–0.69; NIR 0.76–0.9 nm, with uniform response within those ranges). The simulated responses were then used to calculate band indices to capture the development of the plant phenology and stress. For this experiment we considered: uniform 100 nm Green chromatic coordinate ($G/R+G+B$), TM NDVI ($NIR-R/NIR+R$), IR intensity (720–920 nm), camera green chromatic coordinate (G/RGB), 590 nm long-pass blue chromatic coordinate ($IR_B/IR_R+IR_G+IR_B$), and red rejection band pass NDVI ($NIR-B/NIR+B$). All of the indices were calculated as deviation from the initial value to make them more comparable and remove slight individual differences between groups.

3. Results

3.1. Field experiment

Exploratory analysis of image-derived indices showed variation in the correlation between IR indices and greenness-based indices (Table 2), especially for the IR-blue chromatic coordinate. In order to get a more detailed understanding of the sensitivity of these indices to changing illumination and phenological condition we looked at the hourly (Section 3.1.1) and yearly (Section 3.1.2) patterns of



Fig. 3. Setup of the laboratory experiment of a single *Buxus sempervirens* plant in RGB (left) and IR-715 (right). The faded area was excluded when extracting the image data.

Table 2

Correlation matrix (r) for various near-sensing vegetation indices, as derived from the field experiment (Section 3.1).

	Green i	Green Cx	2G-RBi	IR.b i	IR.b Cx	IR 2B-GRI	IR NDVI
Green int.							
Green chr.coord.	-0.07						
2G-RBi	0.40	0.83					
IR.b int.	0.37	0.38	0.40				
IR.b chr.coord.	-0.60	0.56	0.45	-0.08			
IR 2B-GRI	-0.60	0.54	0.44	-0.10	1.00		
IR NDVI	-0.09	0.14	0.11	0.26	0.11	0.11	

three species and compared them to a constant, non-vegetation surface.

3.1.1. Hourly patterns

The hourly profiles of green and *IR* based indices show the yearly averaged values by each hour and corresponding standard deviations (Fig. 5). For the greenness based indices, the 2G-RBi has a much stronger diurnal signal than the *G/RGB* as this index is by design more sensitive to changes in illumination. From the *IR* images, we derived blue channel brightness (sensitive from 800 to 1100 nm) and blue chromatic coordinate (*B/RGB*), which leverages the difference between the blue and other image channels. Again, the blue chromatic coordinate has less hourly variability, indicating a lower sensitivity to illumination changes. In both the greenness and *IR* based indices, different species showed different daily cycles, likely due to shading since the direct illumination varied temporally among the individual plants. This effect is strongest around noon, with highest illumination and therefore strongest contrast between shaded and non-shaded species. Fig. 5 illustrates that the difference between the three plant species and the non-vegetation area is more apparent in the greenness-based indices than in the *IR*-based indices.

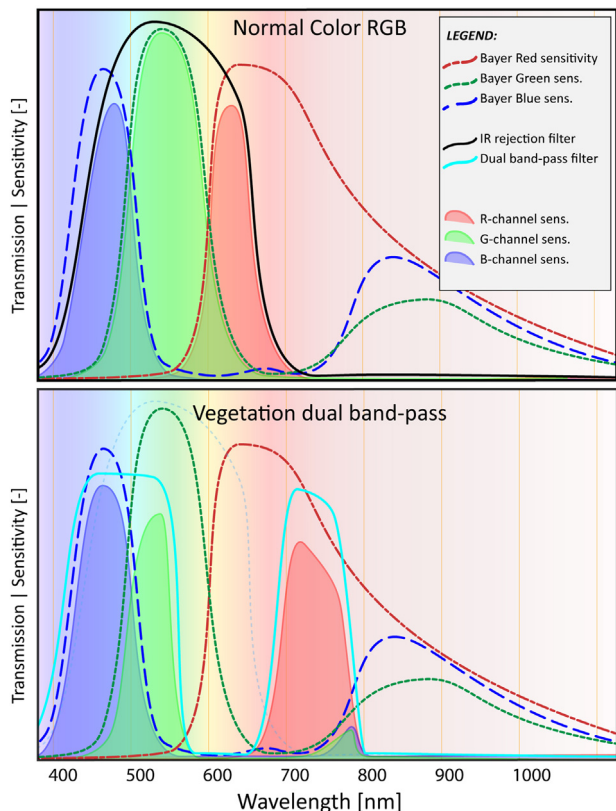


Fig. 4. Idealized filter profiles for a normal (true-color) RGB camera and a camera with a red-rejection dual-band-pass filter as used for the camera simulations.

3.1.2. Yearly development

Fig. 6 shows seasonal trends in our assumedly constant target (wood-chip path), the deciduous bog blueberry (*V. uliginosum*), and the evergreen salal (*G. shallon*). As anticipated, the wood chip shows no clear trend, with most of the small variations likely related to daily illumination conditions. Neither does the *IR_B* chromatic coordinate show any clear trends related to the phenological development of the plants. Conversely, the green chromatic coordinate of the bog blueberry shows a very strong spring leaf flush and decreasing green values as the leaf ages during the growing season. The evergreen salal has high greenness values throughout the year, with a distinct peak during the summer months when new (bright green) leaves unfold. The *IR_B* intensity follows the general trends that can be observed in the greenness, but seems to be less sensitive to the color differences between young and fully developed leaves. The *IR* values show intraday scatter caused by its sensitivity to illumination conditions.

3.2. Laboratory experiment

The spectrometer data from the laboratory experiment allow for a direct comparison of different simulated camera configurations against intensity data and broad band vegetation indices like NDVI. Alongside the spectrometer data, we have validated some simulated camera configurations using a correspondingly modified camera.

NDVI and *G/RGB* are widely used broadband vegetation indices and form a benchmark for the simulated data in this experiment (Fig. 7). They show a pronounced decline in health after day 10 for the drought and drought + heat groups and a less pronounced response for the chlorine and saturation groups. The control and light deprivation groups do not have a clear health response. The stress patterns from these broad band indices correspond to the patterns observed using specific narrowband vegetation indices (de Jong et al., 2012). *IR* intensity shows very similar results as NDVI and *G/RGB*, but with a stronger decline in the saturation and chlorine groups. The simulated camera *G/RGB* has less range than the real camera *G/RGB* because the band separation in a real camera is not optimal. However, the camera *G/RGB* is still able to capture the trends in vegetation health. The *B/RGB* from the 590 nm long pass filter has an extremely small range (note the y-axis) and fails to capture the plant health signal visible in other indices. The red rejection band-pass NDVI shows more variability within the time-series; nevertheless, it captures the general trends in vegetation health well. Both *IR* intensity and *G/RGB* from the actual cameras have a smaller range in their observed changes than the spectrometer data or the simulated camera data, but the general trends in vegetation health are similar (Fig. 8). In contrast to the spectral data, the photos for the light deprivation group did show a decline in health. The response of different test groups is mixed, and where the spectral data shows the strongest response for the drought and drought + heat groups, the photos do not separate them as well. Interpretation of the photo data is somewhat limited by the lack of temporal resolution.

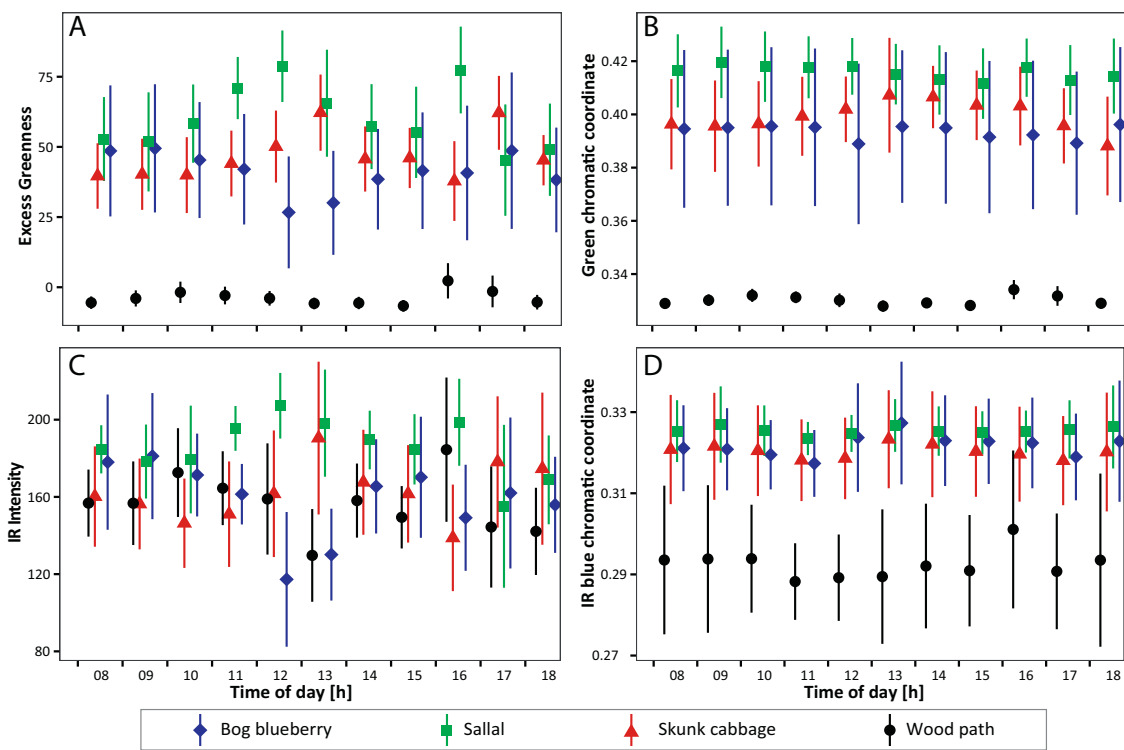


Fig. 5. Hourly patterns of four vegetation indices as averages over the whole year, the lines indicate one standard deviation. Shown are: *V. uliginosum*, Bog blueberry; *G. shallon*, Salal; a *L.americana*, Skunk cabbage; and wood-chip path as non vegetated reference.

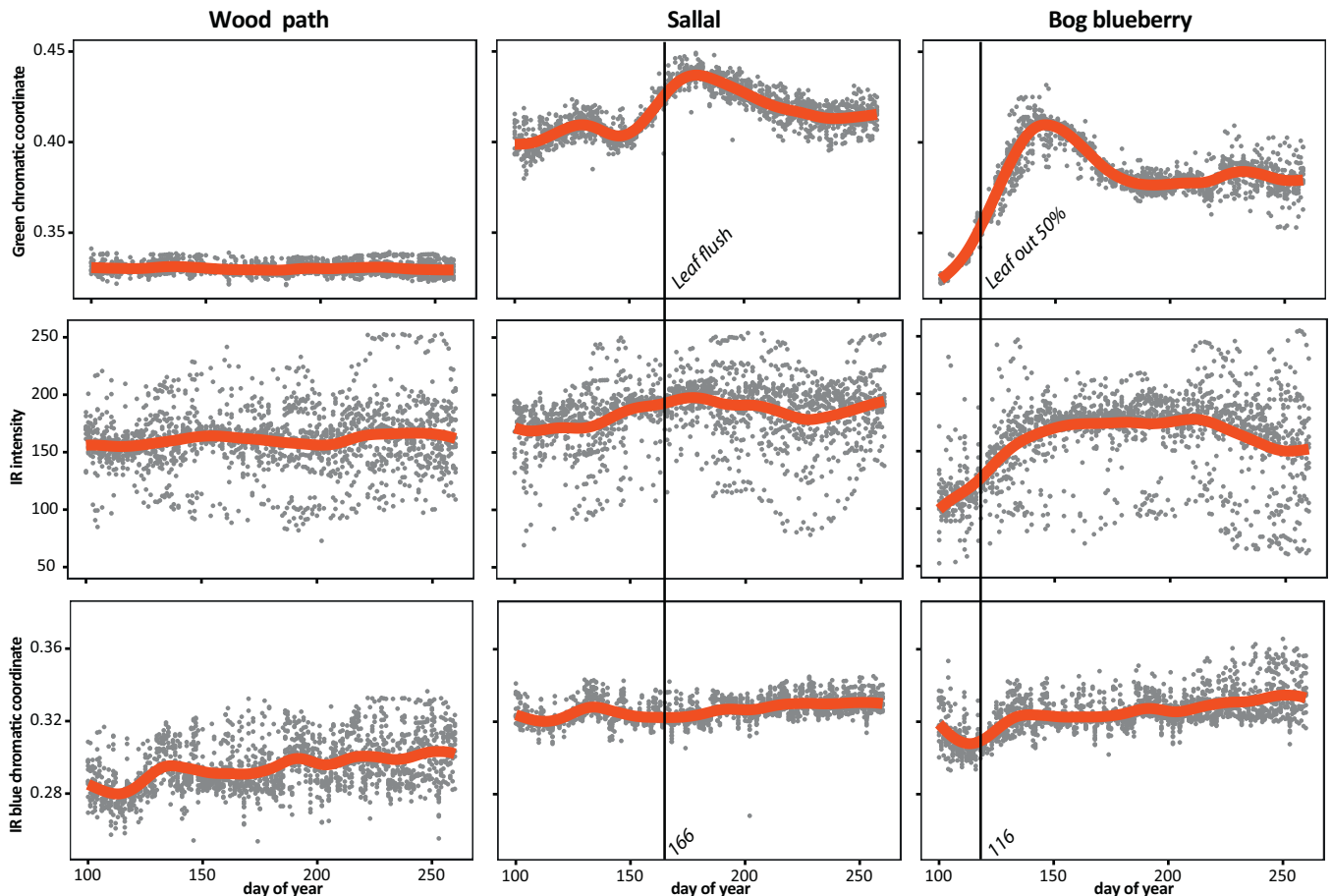


Fig. 6. Yearly patterns and trends for three different vegetation indices for: *V.uliginosum*, Bog blueberry; *G.shallon*, Salal; and the wood path. Key phenological events are marked, for Salal this is the leaf flush is observed at day 166, for Bog blueberry leaf unfolding over 50% was at day 116, senescence was at day 312 falling outside of the graph.

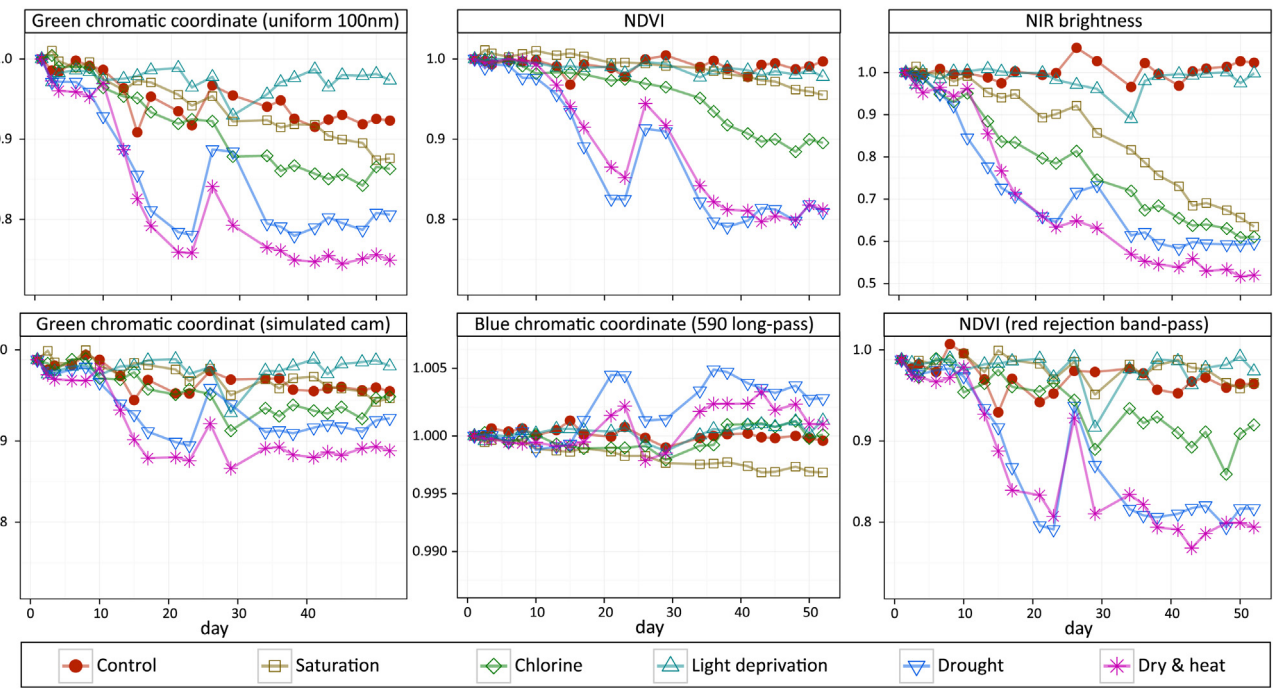


Fig. 7. Trends in plant health as detected by direct (top panels) and simulated (bottom panels) vegetation indices from ASD-fieldspec data over the course of the *Buxus* stress experiment. Standard deviations for each plot are ($n=132$): Green_{100nm}:0.08, NDVI:0.07, NIR_{int} :0.17, Green_{cam}:0.04, Blue_{IR590}:0.002, Red reject NDVI:0.07.

4. Discussion

In this study, we used consumer-grade digital cameras for monitoring plant health and phenology. The performance of near-infrared images was compared against true-color RGB images. The latter were found to outperform infrared images, especially in an uncontrolled (field) environment. The underperformance of infrared imagery for vegetation monitoring is attributable to limitations in dynamic range and band separation. These two issues are discussed below.

The limited dynamic range of consumer grade CCD/CMOS sensors forces the use of camera auto exposure and prevents conversion of digital numbers into calibrated radiance values. If a scene has notable changes in brightness over the monitoring period, the camera has to compensate its exposure, which obscures the detection of actual changes. In complex scenes, local differences in direct versus diffuse illumination may further obscure the changes of interest. Furthermore, consumer cameras apply non-linear transformations to the image data in ways that are beyond user control (Wüller et al., 2007). It is therefore not possible to effectively correct for the changes in illumination and exposure. The lack of calibrated data can be addressed by using color indices that are insensitive to brightness, like the green chromatic coordinate, which is used in many visible-color vegetation studies. In IR cameras that are converted using a long pass filter, such indices have to be constructed using the red and blue channels, leveraging the difference between $IR + Red$ and IR -only information. However, our study shows that the IR_B chromatic coordinate is insensitive to plant health or phenology, both in the field situation and in the lab experiment (Figs. 6 and 7). In the experiments we have considered other band combinations and indices, but none exhibit a clear response in agreement with vegetation trends. Effects of illumination changes can be reduced by selecting images under specific conditions as demonstrated by Ide and Oguma (2010), i.e. using overcast conditions only. However, eliminating images limits data availability and can decrease the temporal resolving power of the analysis.

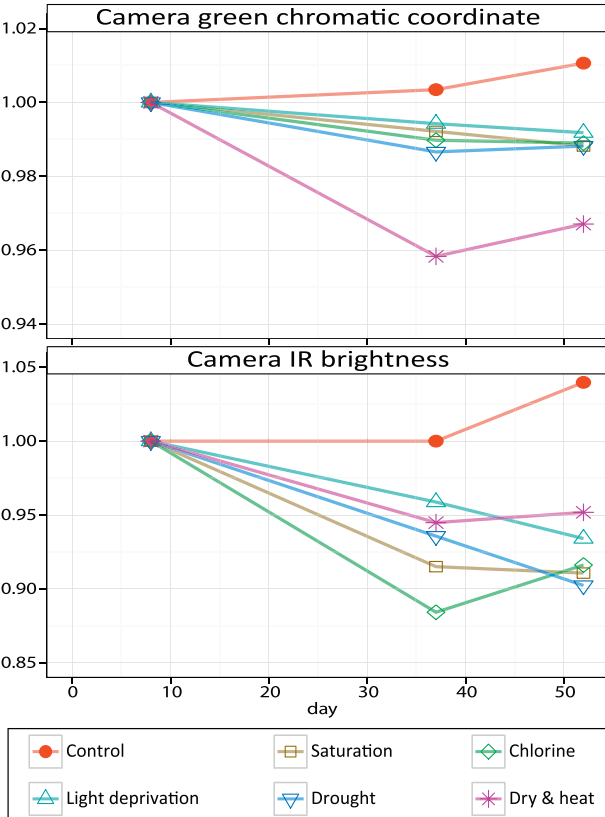


Fig. 8. Trends in plant health as detected by the normal color and 715 nm long pass camera over the course of the *Buxus* stress experiment. Standard deviations for each plot are ($n=24$): Green: 0.001, IR: 0.041.

Table 3

Correlations (r) between the bands in different simulated and theoretical camera configurations for all spectral samples in the laboratory *B. sempervirens* experiment ($n=132$).

Camera configuration	1–2	1–3	2–3
Camera RGB	0.93	0.80	0.66
100 nm Uniform RGB	0.43	0.89	0.50
590 nm Longpass	0.997	0.994	0.996
715 nm Longpass	0.999	0.998	0.997
830 nm Longpass	1.000	1.000	1.000
Red rejection bandpass	0.93	0.17	0.45
TM bands G R NIR	0.14	0.63	-0.64

Sensors in consumer-grade cameras are optimized for true-color RGB recording, which negatively influences the separability of the three channels after infrared conversion. The band configuration is determined by additive rejection of the Bayer filter array and the installed long pass filter (Fig. 1). This results in considerable overlap in sensitivity among the channels and prevents separate recording of red and infrared light. As a result, the bands are highly collinear. Table 3 shows Pearson's correlation between the three bands of different theoretical and simulated camera configurations for all data points in the laboratory stress experiment. The TM bands 2–4 and RGB combinations have intermediate levels of correlation (ranging between 0.1 and 0.9) while all long-pass filter cameras show extreme levels of collinearity (>0.99). This demonstrates the limitation of these cameras to capture more than one dimension of information: brightness. The dual band-pass filter (red rejected) is less affected by collinearity, especially between blue and IR, which makes this configuration a promising option for vegetation studies. For this paper we have not been able to collect extensive data with such a camera but the simulated results in the lab experiment support the interest in this filter type. It must be noted that this camera records only a small part of the near-infrared spectrum, demanding longer exposure times, and lacks a red band. However, but the blue to IR normalized index is likely as close as is it possible to get, given the restrictions of a Bayer color array.

The limitations discussed above apply specifically to a monitoring setting where multiple images are used to create a time series. Several studies show that IR cameras can be effectively used to discriminate between vegetation and other objects within a single image or mosaic of images taken under constant conditions (Aber et al., 2009; Huang et al., 2010; Verhoeven et al., 2009).

5. Conclusions

In this study, we investigated the potential use of IR-sensitive consumer-grade digital cameras for the detection of trends in plant phenology and health in a field situation and during a controlled laboratory experiment. Consumer grade digital cameras are promising tools in monitoring plant health, phenology, and vegetation development at local scales, or by deploying them in a network over larger regions. Results show that IR-converted cameras underperform in a monitoring setting compared to standard color cameras due to these systems' limitations in dynamic range and poor band separation. Simulations show that a conversion with a red-rejection dual-band-pass filter (i.e. blue, green and infrared sensitivity) largely overcomes these issues, making it a promising tool for vegetation monitoring studies. Consumer-grade RGB cameras are already widely used in vegetation monitoring settings and our results further support and promote their use as simple and affordable tools for reliable detection and monitoring of plant stress, development and phenology.

Acknowledgments

The authors would like to thank Daniel Mosquin of the UBC Botanical Garden and Andrew Riseman of the UBC Farm for their cooperation in the camera field experiment. Priscilla Hoogenboom is acknowledged for her contributions to the laboratory stress study. The study was supported by the Grizzly bear program of the Foothills Research Institute.

References

- Aber, J.S., Aber, S.W., Buster, L., Jensen, W.E., Sleezer, R.L., 2009. Challenge of infrared kite aerial photography: a digital update. *Trans. Kans. Acad. Sci.* 112, 31–39.
- Badeck, F.W., Bondeau, A., Bottcher, K., Doctor, D., Lucht, W., Schaber, J., Sitch, S., 2004. Responses of spring phenology to climate change. *New Phytol.* 162, 295–309.
- Bale, J.S., Masters, G.J., Hodkinson, I.D., Awmack, C., Bezemer, T.M., Brown, V.K., Butterfield, J., Buse, A., Coulson, J.C., Farrar, J., Good, J.E.G., Harrington, R., Hartley, S., Jones, T.H., Lindroth, R.L., Press, M.C., Symrnioudis, I., Watt, A.D., Whittaker, J.B., 2002. Herbivory in global climate change research: direct effects of rising temperature on insect herbivores. *Global Change Biol.* 8, 1–16.
- Bater, C., Coops, N., Wulder, M., Hilker, T., Nielsen, S., McDermid, G., Stenhouse, G.B., 2011a. Using digital time-lapse cameras to monitor species-specific understorey and overstorey phenology in support of wildlife habitat assessment. *Environ. Monit. Assess.* 180, 1–13.
- Bater, C., Coops, N.C., Wulder, M.A., Nielsen, S.E., McDermid, G., Stenhouse, G., 2011. Design and installation of a camera network across an elevation gradient for habitat assessment. *Instrum. Sci. Technol.* 39, 231–247.
- Bauer, S.D., Korč, F., Förstner, W., 2011. The potential of automatic methods of classification to identify leaf diseases from multispectral images. *Precision Agric.* 12, 361–377.
- Bayer, B.E., 1976. Color imaging array. In: US Patent 3971065. Eastman Kodak Company, Rochester, NY.
- Brooker, G., 2009. Introduction to Sensors for Ranging and Imaging. SciTech Publishing, NC, USA.
- Buil, C., 2012. IR-Cut Filter Removal Operation, Performances and Image Samples, (<http://www.astrosurf.com/buil/350d/350d.htm>) [access 2012/12/11].
- Cleland, E.E., Chuique, I., Menzel, A., Mooney, H.A., Schwartz, M.D., 2007. Shifting plant phenology in response to global change. *Trends Ecol. Evol.* 22, 357–365.
- Coops, N.C., Hilker, T., Bater, C., Wulder, M.A., Nielsen, S.E., McDermid, G., Stenhouse, G., 2012. Linking ground-based to satellite-derived phenological metrics in support of habitat assessment. *Remote Sens. Lett.* 3, 191–200.
- Dierschke, H., 1972. Zur Aufnahme und Darstellung phänologischer Erscheinungen in Pflanzengesellschaften. In: Wessell, R.E., Talbot, S.S. (Eds.), 1970 International Symposium for Vegetation Science. The Hague.
- Fisher, J.I., Mustard, J.F., Vadéboncoeur, M.A., 2006. Green leaf phenology at Landsat resolution: scaling from the field to the satellite. *Remote Sens. Environ.* 100, 265–279.
- Graham, E.A., Riordan, E.C., Yuen, E.M., Estrin, D., Rundel, P.W., 2010. Public internet-connected cameras used as a cross-continental ground-based plant phenology monitoring system. *Global Change Biol.* 16, 3014–3023.
- Hirakawa, K., Wolfe, P.J., 2008. Spatio-spectral sampling and color filter array design. In: Lukac, R. (Ed.), Single-Sensor Imaging: Methods and Applications for Digital Cameras. CRC Press, Boca Raton, FL.
- Huang, Y., Thomson, S.J., Lan, Y., Maas, S.J., 2010. Multispectral imaging systems for airborne remote sensing to support agricultural production management. *Int. J. Agric. Biol. Eng.* 3, 50–62.
- Hufkens, K., Friedl, M., Sonnentag, O., Braswell, B.H., Milliman, T., Richardson, A.D., 2012. Linking near-surface and satellite remote sensing measurements of deciduous broadleaf forest phenology. *Remote Sens. Environ.* 117, 307–321.
- Ide, R., Oguma, H., 2010. Use of digital cameras for phenological observations. *Ecol. Inf.* 5, 339–347.
- Jacobs, N., Burgin, W., Fridrich, N., Abrams, A., Miskell, K., Braswell, B., Richardson, A.D., Pless, R., 2009. The global network of outdoor webcams: properties and applications. In: Networks. ACM International Conference on Advances in Geographic Information Systems, Seattle, WA, pp. 111–120.
- de Jong, S.M., Addink, E.A., Hoogenboom, P., Nijland, W., 2012. The spectral response of *Buxus sempervirens* to different types of environmental stress—a laboratory experiment. *ISPRS J. Photogramm. Remote Sens.* 74, 56–65.
- Jongschaap, R.E.E., Booij, R., 2004. Spectral measurements at different spatial scales in potato: relating leaf, plant and canopy nitrogen status. *Int. J. Appl. Earth Obs. Geoinf.* 5, 205–218.
- Knoth, C., Prinz, T., Loef, P., 2010. Microcopter-based color infrared (CIR) close range remote sensing as a subsidiary tool for precision farming. In: Proceedings of the Workshop on Remote Sensing Methods for Change Detection and Process Modelling, pp. 49–54.
- Konica, Minolta, 1998. Precise Color Communication. Konica Minolta Sensing Inc, Osaka, Japan.
- Kurc, S., Benton, a.L.M., 2010. Digital image-derived greenness links deep soil moisture to carbon uptake in a creosotebush-dominated shrubland. *J. Arid. Environ.* 74, 585–594.
- LDP LCC, 2012. Spectral Response, (<http://maxmax.com/spectral.response.htm>) [access 2012/12/11].

- Lelong, C.C.D., 2008. Assessment of unmanned aerial vehicles imagery for quantitative monitoring of wheat crop in small plots. *Sensors* 8, 3557–3585.
- Liang, L., Schwartz, M.D., Fei, S., 2011. Validating satellite phenology through intensive ground observation and landscape scaling in a mixed seasonal forest. *Remote Sens. Environ.* 115, 143–157.
- Linderholm, H.W., 2006. Growing season changes in the last century. *Agric. For. Meteorol.* 137, 1–14.
- Markham, B.L., Helder, D.L., 2011. Forty-year calibrated record of earth-reflected radiance from landsat: a review. *Remote Sens. Environ.* 12230–12240, 2012.
- Nielsen, S., Boyce, M., Stenhouse Gordon, B., Munro, R.H.M., 2003. Development and testing of phenologically driven grizzly bear habitat models. *Ecoscience* 10, 1–10.
- Nielsen, S.E., McDermid, G., Stenhouse, G.B., Boyce, M.S., 2010. Dynamic wildlife habitat models: seasonal foods and mortality risk predict occupancy-abundance and habitat selection in grizzly bears. *Biol. Conserv.* 143, 1623–1634.
- Nijland, W., Coops, N.C., Coogan, S.C.P., Bater, C.W., Wulder, M.A., Nielsen, S.E., McDermid, G., Stenhouse, G.B., 2012. Vegetation phenology can be captured with digital repeat photography and linked to variability of root nutrition in *Hedysarum alpinum*. *Appl. Veg. Sci.* 16, 317–324.
- Nijland, W., 2012. Basics of Infrared Photography, Infrared light, (http://www.ir-photo.net/ir_imaging.html) [access 2012/12/11].
- Papeş, M., Peterson, A.T., Powell, G.V.N., 2012. Vegetation dynamics and avian seasonal migration: clues from remotely sensed vegetation indices and ecological niche modelling. *J. Biogeogr.* 39, 652–664.
- Polgar, C.A., Primack, R.B., 2011. Leaf-out phenology of temperate woody plants: from trees to ecosystems. *New Phytol.* 191, 926–941.
- Post, E., Stenseth, N., 1999. Climatic variability, plant phenology, and northern ungulates. *Ecology* 80, 1322–1339.
- Poynton, C., 1995. A guided tour of color space. In: Proceedings of the SMPTE Advanced Television and Electronic Imaging Conference, New Foundations for Video Technology, San Francisco, Feb. 1995, pp. 167–180.
- Richardson, A.D., Braswell, B.H., Hollinger, D.Y., Jenkins, J.P., Ollinger, S.V., 2009. Near-surface remote sensing of spatial and temporal variation in canopy phenology. *Ecol. Appl.* 19, 1417–1428.
- Richardson, A.D., Jenkins, J.P., Braswell, B.H., Hollinger, D.Y., Ollinger, S.V., Smith, M.L., 2007. Use of digital webcam images to track spring green-up in a deciduous broadleaf forest. *Oecologia* 152, 323–334.
- Sharma, S., Couturier, S., Côté, S.D., Cote, S.D., 2009. Impacts of climate change on the seasonal distribution of migratory caribou. *Global Change Biol.* 15, 2549–2562.
- Sonnentag, O., Hufkens, K., Teshera-Sterne, C., Young, A.M., Friedl, M., Braswell, B.H., Milliman, T., O'Keefe, J., Richardson, A.D., 2012. Digital repeat photography for phenological research in forest ecosystems. *Agric. For. Meteorol.* 152, 159–177.
- Soudani, K., Hmimina, G., Delpierre, N., Pontailler, J.-Y., Aubinet, M., Bonal, D., Caquet, B., De Grandcourt, A., Burban, B., Flechard, C., Guyon, D., Granier, A., Gross, P., Heinesh, B., Longdoz, B., Loustau, D., Moureaux, C., Ourcival, J.-M., Rambal, S., Saint André, L., Dufrêne, E., 2012. Ground-based network of NDVI measurements for tracking temporal dynamics of canopy structure and vegetation phenology in different biomes. *Remote Sens. Environ.* 123, 234–245.
- Tucker, C.J., 1979. Red and photographic infrared linear combinations for monitoring vegetation. *Remote Sens. Environ.* 8, 127–150.
- Verhoeven, G.J., Loenders, J.O., Vermeulen, F., Docter, R., 2009. Helikite aerial photography—a versatile means of unmanned, radio controlled, low-altitude aerial archaeology. *Archaeol. Prospect.* 16, 125–138.
- Verhoeven, G.J.J., 2010. It's all about the format—unleashing the power of RAW aerial photography. *Int. J. Remote Sens.* 31, 2009–2042.
- Woebbecke, D.M., Meyer, G.E., Von Bargen, K., Mortensen, D.A., 1995. Color indices for weed identification under various soil, residue, and lighting conditions. *Trans. Am. Soc. Agric. Eng.* 38, 259–269.
- Wüller, D., Gabele, H., Electronic, F., GmbH, V.C.Z.H., 2007. The usage of digital cameras as luminance meters. *Image Eng.* 6502, 1–11.
- Zhang, X., Friedl, M.A., Schaaf, C.B., Strahler, A.H., Hodges, J.C.F., Gao, F., Reed, B., Huete, A., 2003. Monitoring vegetation phenology using MODIS. *Remote Sens. Environ.* 84, 471–475.